CHAPTER VI

DISCUSSION AND CONCLUSION

To obtain the numerical value of $m\mu_0$ and ρ_c/ρ respectively, we have used interaction the Lennard-Jones 12-6 potential, the Morse-V_{DD} potential, and the HFDHE-2 potential. These interatomic potentials are claimed to give the best fit for ^{4}He II system, since their virial coefficients are in agreement with the experimental results. However, difficultlies arise, when the interatomic distance r between neutral helium atoms approaches zero.

In the field theoretical approaches(2,27,28) to ^{4}He II problem, one takes Fourier transform of the interatomic potential into the momentum space. The L-J 12-6 potential give the divergent result when transformed into the momentum space while the Morse-V_{DD} potential and the HFDHE-2 potential yield the convergent results as shown H H.R Glyde(25). For the example, the Fourier transform of the L-J 12-6 potential, the Morse-V_{DD} potential and the HFDHE-2 potential, for momentum $\vec{k} = 0$, are

$$V_{L-J}(\vec{k} = 0) \quad = \quad 16\pi\varepsilon\int_0^\infty \{(r_0/r)^{12} - (r_0/r)^6\}r^2dr \quad = \quad \infty \qquad (6\text{-}1)$$

$$V_{M-V_{DD}}(\vec{k}) \quad = \quad \frac{4\pi}{k}\int_0^\infty V(r)\sin(kr).rdr \quad = \quad a + bk^2 + ck^4 \qquad (6\text{-}2)$$

$$(V_{M-V_{DD}}(\vec{k} = 0) \quad = \quad a \quad = \quad 7.4093)$$

where $a = 7.4093$; $b = -0.73407$; $c = 0.000628$

and

$$V_{H-2}(\vec{k} = 0) = 4\pi\varepsilon\int_0^\infty \Big[A\exp(-\alpha_1 r/r_m) - \{C_6(r_m/r)^6 + C_8(r_m/r)^8 + C_{10}(r_m/r)^{10}\}F(r)\Big] r^2 dr \qquad (6-3)$$

where equation (6-3) yield the convergent result. In the calculation of energy spectrum for liquid ^{4}He II and of condensate density below T_λ, $V(\vec{k})$ is very important, since it is always presents in the microscopic theories(2).

In Table I and Table II, the numerical value of the ground state energy and the condensate fraction of liquid ^{4}He II at T = 0 K are shown along with those of other works. In the calculation, equations (4-23) and (4-55) have been used to get the numerical value of $m\mu_0$ and ρ_c/ρ, where we have assumed that the screening factor $\$_1(\vec{r}) = \$_2(\vec{r})$ (without any justification). The experimental work of Sears(26), Lam and Ristig(11), and the proposal of Cummings et.al(18) tends to support this assumption. In the calculation, the area under curves of I^α, I^β and I^μ vs r were obtained with Simpson's rule method, we have seen that the calculation are sensitive to the behaviour of the function $\$(\vec{r})$, $h(\vec{r})$ and the value of ρ_c/ρ. Theoretical estimates of ρ_c/ρ by Sears(26) recently shows that $\rho_c/\rho = 0.139\pm0.023$. These values of ρ_c/ρ would change the value of the ground state energy greatly.

6.1 Ground State Energy

We first obtained our numerical results by using the data from curve of McMillan. The L-J 12-6 potential and the Morse-V_{DD} potential were seen to yield the value of the ground state energy which were in good agreement with those of others(2,13). The HFDHE-2 potential did not yield good results. Next we use data from the curve of HNCE scaling in replace of data from the McMillan'curve. The L-J 12-6 potential, the Morse-V_{DD} potential, and the HFDHE-2 potential were found to yield the values of the ground state enrgy which were in good agreement with those of other. Use of the curve of Puoskari yield better value than the use of McMillan's curve.

Since our theoretical considerations were not concern to the Fourier transform, the divergence or non divergence difficulties did not enter into our calculation. Our results cannot be used to decide which potential is the most appropriate for ^4He. The most appropriate interatomic potential in liquid ^4He is still being sought.

6.2 Condensate Fraction

In Table II, our results(obtained from of McMillan's curve) for the L-J 12-6 potential, the Morse-V_{DD} potential, and the HFDHE-2 potential, show that the value of the condensate fraction not good. We have also used data of the HNCE scaling in replace the McMillan's data. The numerical value of the condensate fraction at 0 K obtained from the Morse-V_{DD} potential is in good agreement with others, whereas the L-J 12-6 potential and the HFDHE-2 potential are not.

For the value of the condensate fraction, our results are obtained from equation (4-55), where α and β are calculated at 0 K. We have curves of ρ vs T using data from McMillan's curve and from HNCE scaling curve (Fig.6.2 and Fig.6.3), we have compared the new ρ vs T curve with those obtained by Visoottiviseth(30) and by Sears(26) in Fig.6.1. From Table II, we see that the results of the condensate fraction at 0 K which have been calculated are not good. We expect (4-55) the exact relationship between ρ_c and ρ_s is not given by equation (4-55). Sears et.al(21) have found the structure factor and the pair-correlation function by the neutron scattering method and they have used the equation (4-45) proposed by Cummings et.al(18) in obtaining the condensate fraction which is in agreement with the other theoretical work. They obtain

$$\rho_c(T) \quad = \quad \rho_c(0)\left[1 - (T/T_\lambda)^a\right] \qquad (6-4)$$

where $\rho_c(0)/\rho \quad = \quad 0.133\pm0.012 \ ; \quad a \quad = \quad 4.7\pm1.2$

Visoottiviseth(30) has proposed the relationship between the condensate density and the superfluid density

$$\rho_c(T) \quad = \quad \gamma(T)\rho_s(T) \qquad (6-5)$$

6.2.1 Near T_λ

Near the λ-point(T_λ = 2.17), Wong(33) and Tyson et.al(34) have found that

$$\rho_s \sim (1 - T/T_\lambda)^{2/3} \qquad (6-6)$$

$$\rho_c \sim (1 - T/T_\lambda) \qquad (6-7)$$

thus

$$\gamma(T) \sim (1 - T/T_\lambda)^{1/3} \qquad (6-8)$$

We see that the screening factor $\$(\vec{r})$ and the function $h(\vec{r})$ depend on the temperature. If we know the exact form of the screening factor $\$(\vec{r},T)$ and the function $h(\vec{r},T)$, we could obtain the values of condensate fraction which would be in better agreement with the experimental value of Sears et.al(21).

The function $h(r,T)$ might be the gaussion function,

$$h(r,T) = e^{-ar^2/(T_\lambda - T)} \qquad (6-9)$$

where a is the parameter fitted to the curve at 0 K. When T approaches T_λ, the function

$$h(r,T) \xrightarrow[T \to T_\lambda]{} 0$$

and when $r \longrightarrow 0$, we then obtain

$$h(r=0,T) \longrightarrow 1$$

as it should be. Therefore the function $h(\vec{r},T)$ might be used to denote the onset of criterion of superfluidity of He II.

6.2.2 Near T = 0 K

From equation (6-4), T = 0 K, we obtain

$$\rho_c(T = 0\ K) = \rho_c(0) = 0.133 \pm 0.012 .$$

T = o K, we have equation (6-5)

$$\rho_c(T = 0\ K) = \gamma(T = 0\ K)\rho ,$$

where $\rho_s(T) \xrightarrow[T \to 0\ K]{} \rho$. According to Creswick(35)

$$\rho_s(T) = \rho(1 - AT^4) , \qquad T \simeq 0\ K . \qquad (6\text{-}10)$$

We can obtain from equations (6-4), (6-5), and (6-10)

$$\gamma(T) = \frac{\rho_c(0)}{\rho}\left[\frac{1 - CT^a}{1 - AT^4}\right] \xrightarrow[T \to 0]{} \rho_c(0)/\rho \qquad (6\text{-}11)$$

This equation is for the condensate fraction depend on the temperature.

The validity of the two-fluid model is most strikingly demonstrated in the experiment devised by Andronikashvili(1946). He used a pile of equally spaced thin metal disks(Fig.6.4), suspensed by a torsion fibre so that they were able to perform oscillation in liquid helium. The disk spacing was sufficiently small to ensure that above T_λ all the fluid between the disks was dragged with them. However, below T_λ the period of oscillation decreased sharply, indicating that not all the fluid in the spaces was being entrained by the disks. This result confrimed the prediction that the superfluid fraction would have no effect on the torsion pendulum. The experiment yields a direct method of measuring the variation of ρ_n/ρ with temperature (Fig.6.4), and by inference ρ_s/ρ. We note that He II is almost entirely superfluid below 1 K. From Fig.6.4, we expect the equation from curve of ρ_s/ρ is

$$\frac{\rho_s(T)}{\rho} = \left[1 - (T/T_\lambda)^m\right] \qquad (6\text{-}12)$$

where we can find the constant m by fitting the variation of temperature T with ρ_s/ρ. We thus obtain the expression of relationship between the condensate density and the superfluid density

$$\frac{\rho_c(T)}{\rho} = \gamma(T)\frac{\rho_s(T)}{\rho}. \qquad (6\text{-}13)$$

From equations (6-12) and (6-13) we obtain

$$\frac{\rho_c(T)}{\rho} = \gamma(T)\left[1 - (T/T_\lambda)^m\right] \qquad (6\text{-}14)$$

when $T \longrightarrow 0$, we thus obtain from equation (6-14)

$$\frac{\rho_c}{\rho} \xrightarrow[T \longrightarrow 0]{} \gamma(0)$$

6.3 Second Order Reduced Density Matrix Ω_2

A number of general physical relations valid for system consisting of a great number of particles must be derivable from microphysics in a manner which does not make use of detailed solutions of the N-body problem. One set of such general features are connected with the so-called reduced density matrices. From the exact equations of motion of the first and second reduced density matrices and in conjunction with the some general symmetry properties of such matrices, Fröhlich(17,36,37) derived the generally valid equations of hydrodynamics and the equations of motion of some macroscopic wave function, without resorting to a specific microscopic model.

Cummings et.al(18) proposed for an experimental determination of the equilibrium condensate fraction in ^{4}He II which relies only on measurement of the liquid structure factor as a function of temperature. The equilibrium pair-correlation function at temperature T, P(r,T) can be written in terms of the second order reduced density matrix Ω_2 as

$$P(r,T) = \Omega_2(\vec{x},\vec{y};\vec{x},\vec{y}|T) = \rho_c^2(T) + 2\rho_c(T)\rho_d + \Lambda_2(r,T)$$

P(r,T) is, however, directly related to the experimentally determinable quality the radial distribution function, g(r,T), by

$$P(r,T) = \Omega_2(\vec{x},\vec{y};\vec{x},\vec{y}|T) = N^2 g(r,T)$$

then for $T < T_\lambda$

$$\frac{\rho_c}{\rho}(T) = 1 - \left[\frac{g(r,T) - 1}{g(r,T=T_\lambda) - 1}\right]^{1/2} \qquad (6\text{-}15)$$

Cummings(22) has discussed the piloting action of the macroscopic wave function in a superfluid at T = 0 K, by using a principle of an approximate expression of the energy.

Terreaux and Lal(24) have improved the form of the second reduced density matrix by using a relevant assumption.

Griffin(38) has discussed some simple models for a condensed-Bose system (free particles and the Bogoliubov model for a dilute interacting Bose gas) and make contact with the work of Fröhlich(17) as well as Hyland, Rowlands, and Cummings(14,18).

Yukalov(39) has shown that for the model of a condensate with non-zero momentum satisfies the Hyland, Rowlands, and Cummings formula.

Finally, Ghassib and Sridhar(40) have shown a new simple formula for determining condensate fraction in He II, where he has begun with the familar equation for Ω_1 and Ω_2

$$\Omega_1(\vec{r}_1', \vec{r}_1) = \rho_c N + \Lambda_1(\vec{r}_1' - \vec{r}_1); \quad (6\text{-}16)$$

$$\Omega_2(\vec{r}_1', \vec{r}_2'; \vec{r}_1, \vec{r}_2) = \Omega_1(\vec{r}_1', \vec{r}_1)\Omega_1(\vec{r}_2', \vec{r}_2) + \Omega_1(\vec{r}_1', \vec{r}_2)\Omega_1(\vec{r}_2', \vec{r}_1) - \rho_c^2 N^2 + \Omega_2(\vec{r}_1', \vec{r}_2'; \vec{r}_1, \vec{r}_2). \quad (6\text{-}17)$$

Invoking the usual definition for $g(\vec{r}_1 - \vec{r}_2) = g(\vec{r})$

$$\Omega_2(\vec{r}_1, \vec{r}_2; \vec{r}_1, \vec{r}_2) = N^2 g(\vec{r}_1 - \vec{r}_2), \quad (6\text{-}18)$$

upon combining equations (6-16) and (6-17)

$$g(\vec{r}_1 - \vec{r}_2) = 1 - \rho_c^2 + |\Omega_1(\vec{r}_1\vec{r}_2)|^2/ N^2 + \Lambda_2(\vec{r}_1\vec{r}_2;\vec{r}_1\vec{r}_2)/N^2. \tag{6-19}$$

He thus obtains from equation (6-19)

$$\rho_c = \frac{1}{2} \lim_{r \to \infty} \left| \frac{\Lambda_2(\vec{r})}{\Lambda_1(\vec{r})} \right|, \tag{6-20}$$

which we would like to point out that this expression (6-20) is not exactly. But it should be

$$\rho_c = \frac{1}{2N} \lim_{r \to \infty} \left(\frac{-\Lambda_2(\vec{r}) - \Lambda_1^2(\vec{r})}{\Lambda_1(\vec{r})} \right). \tag{6-21}$$

However, neither the equation (6-20) nor (6-21) yields the numerical value of $\rho_c(T)$.

Finally, we believes that our expression for Ω_2 (eq. (4-12)) is a reasonable one.

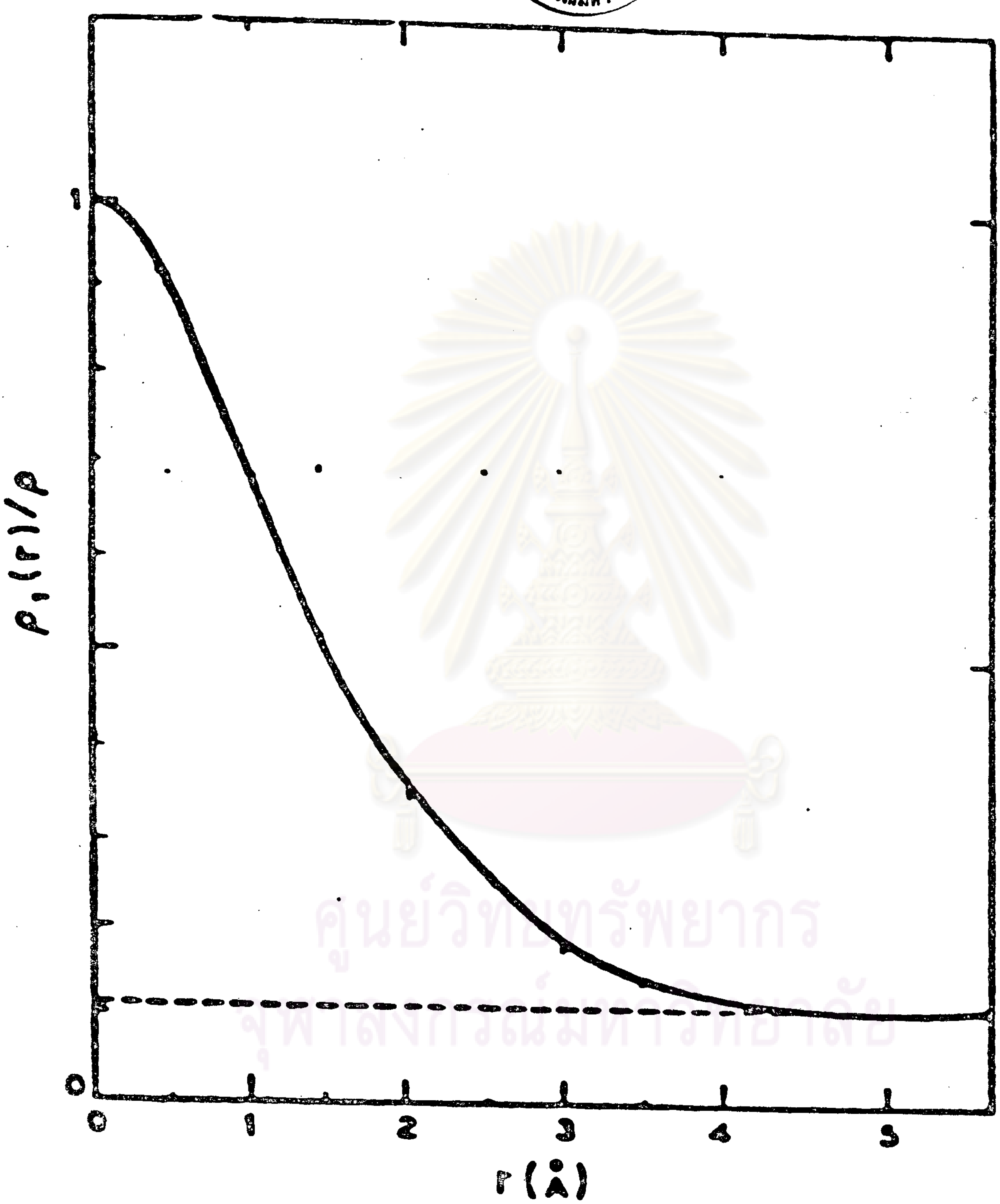

Fig 5.1 This figure is McMillan' curve.

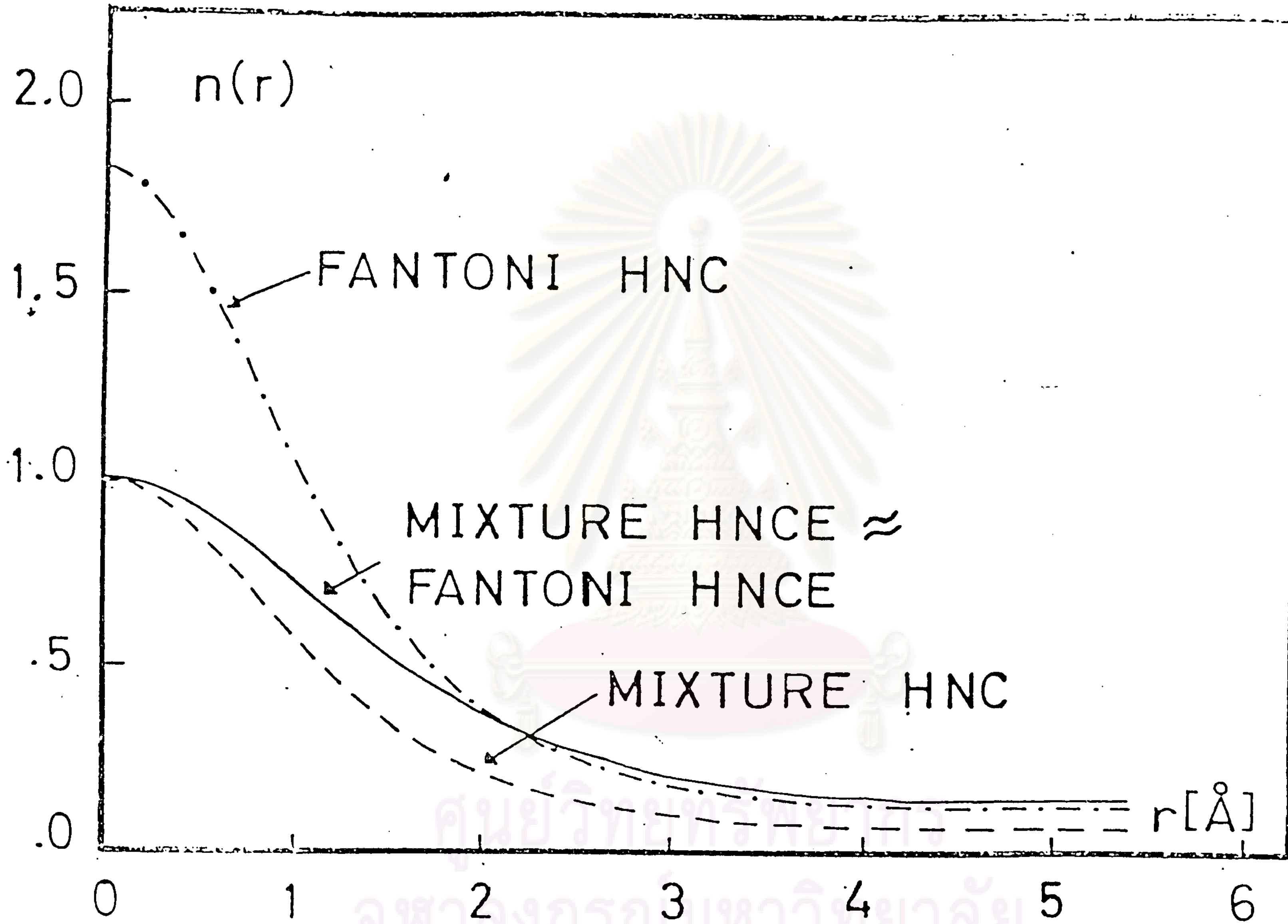

Fig 5.2 This figure is HNCE scaling

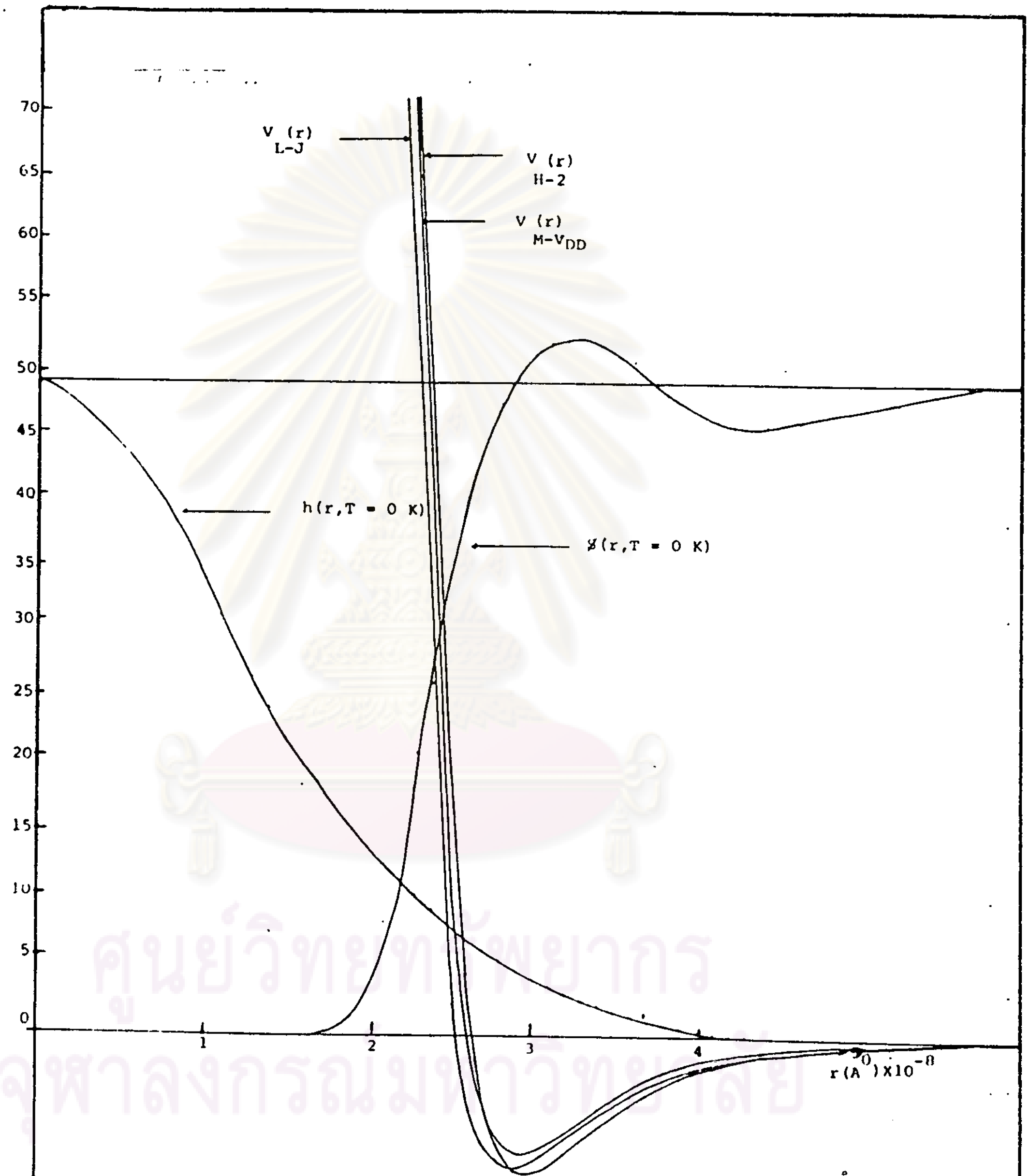

FIG 5-3 The Lennard-Jones 12-6 potential, $V_{L-J}(r)$, The Morse-V_{DD} potential $V_{DD}(r)$, and The HFDHE 2, $V_{H-2}(r)$, in unit of 25×10^{-2} K, the screening function $\phi_1(r,T=0\ K)$ and the function $h(r,T=0\ K)$ computed from McMillan 's curve

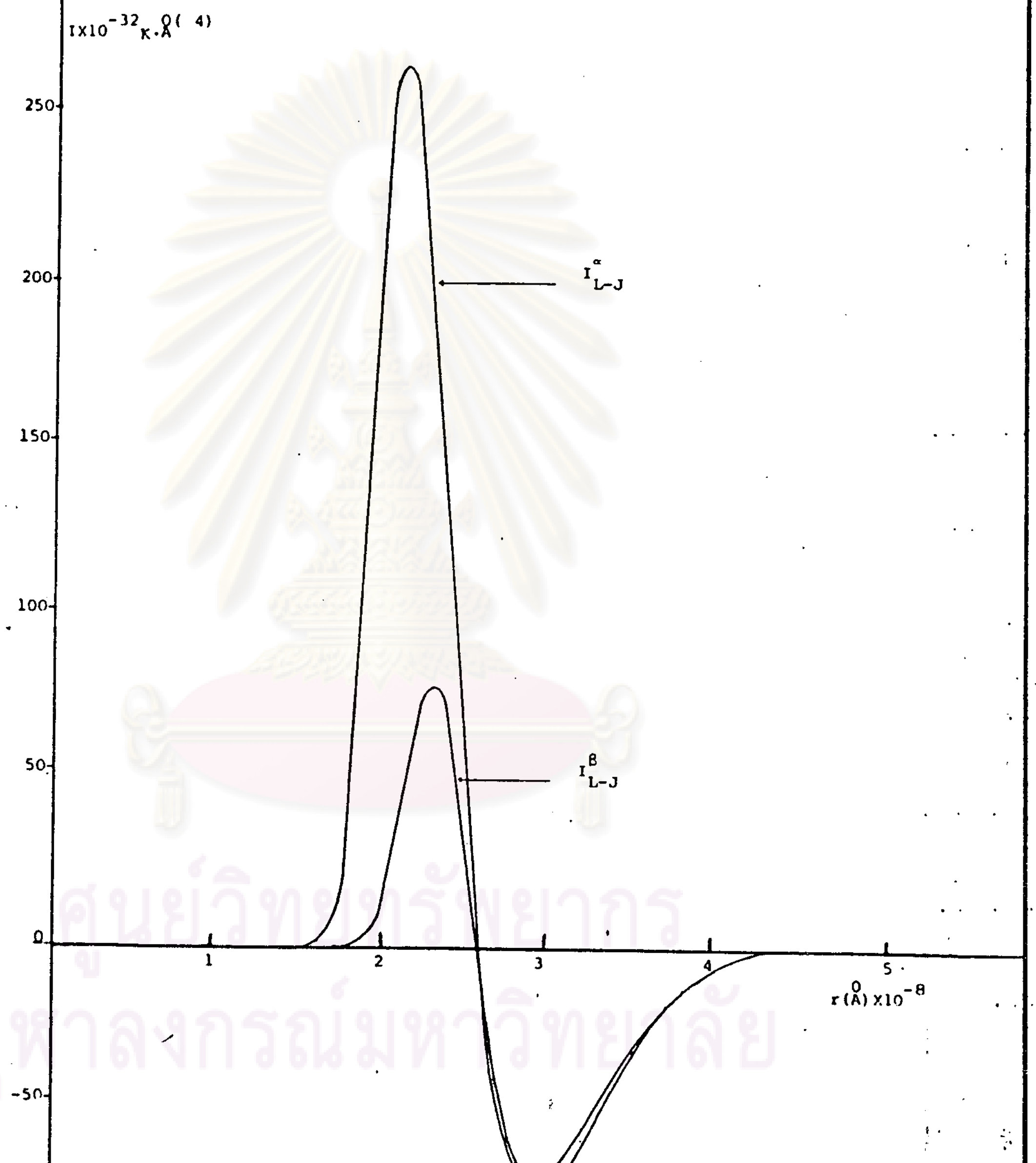

FIG 5-4 I^{α}_{L-J} and I^{β}_{L-J} VS r, due to the L-J 12-6 potential, which have been computed from McMillan's curve

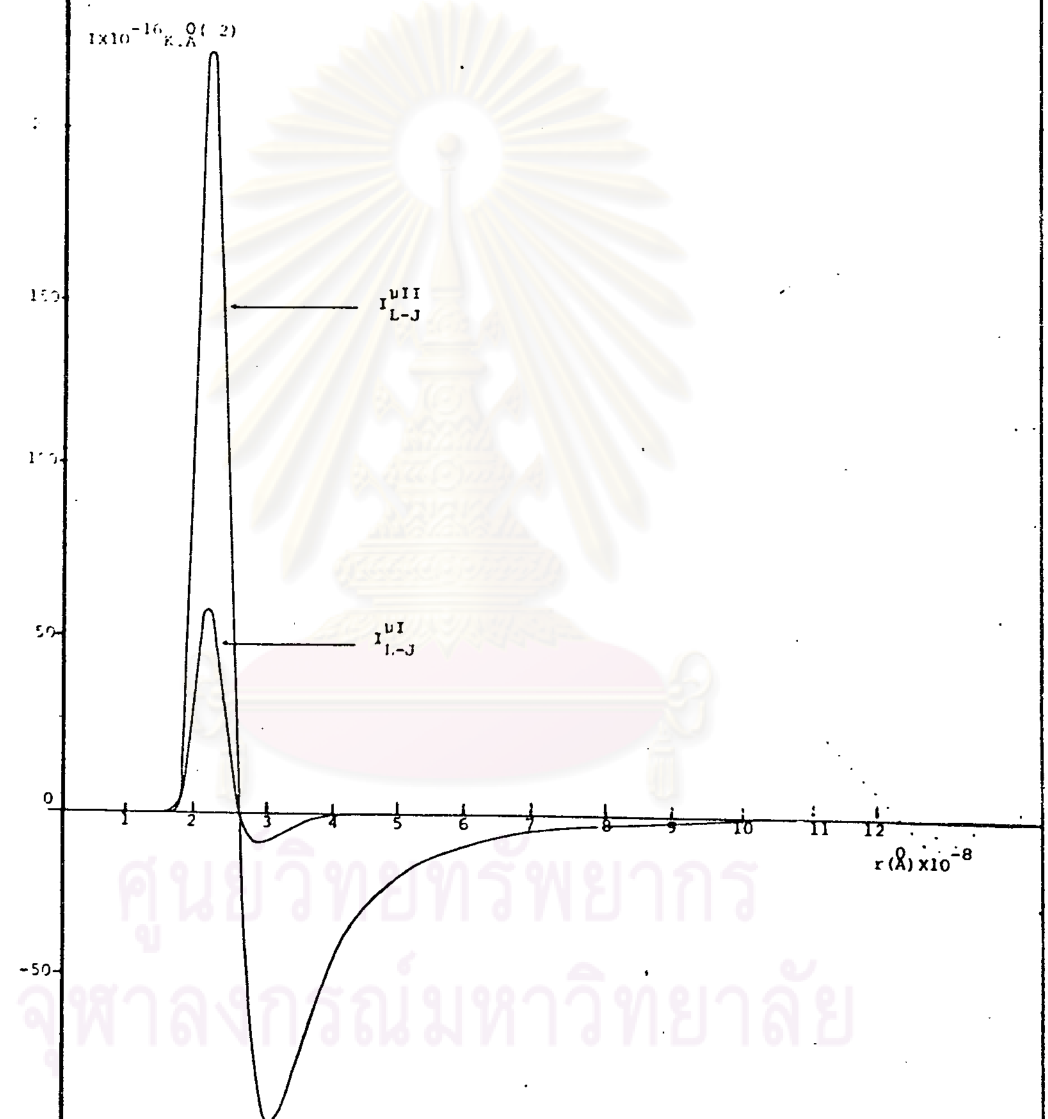

FIG 5-5 $I^{\mu I}_{L-J}$ and $I^{\mu II}_{L-J}$ VS r, due to the L-J 12-6 potential, which have been computed from McMillan's curve

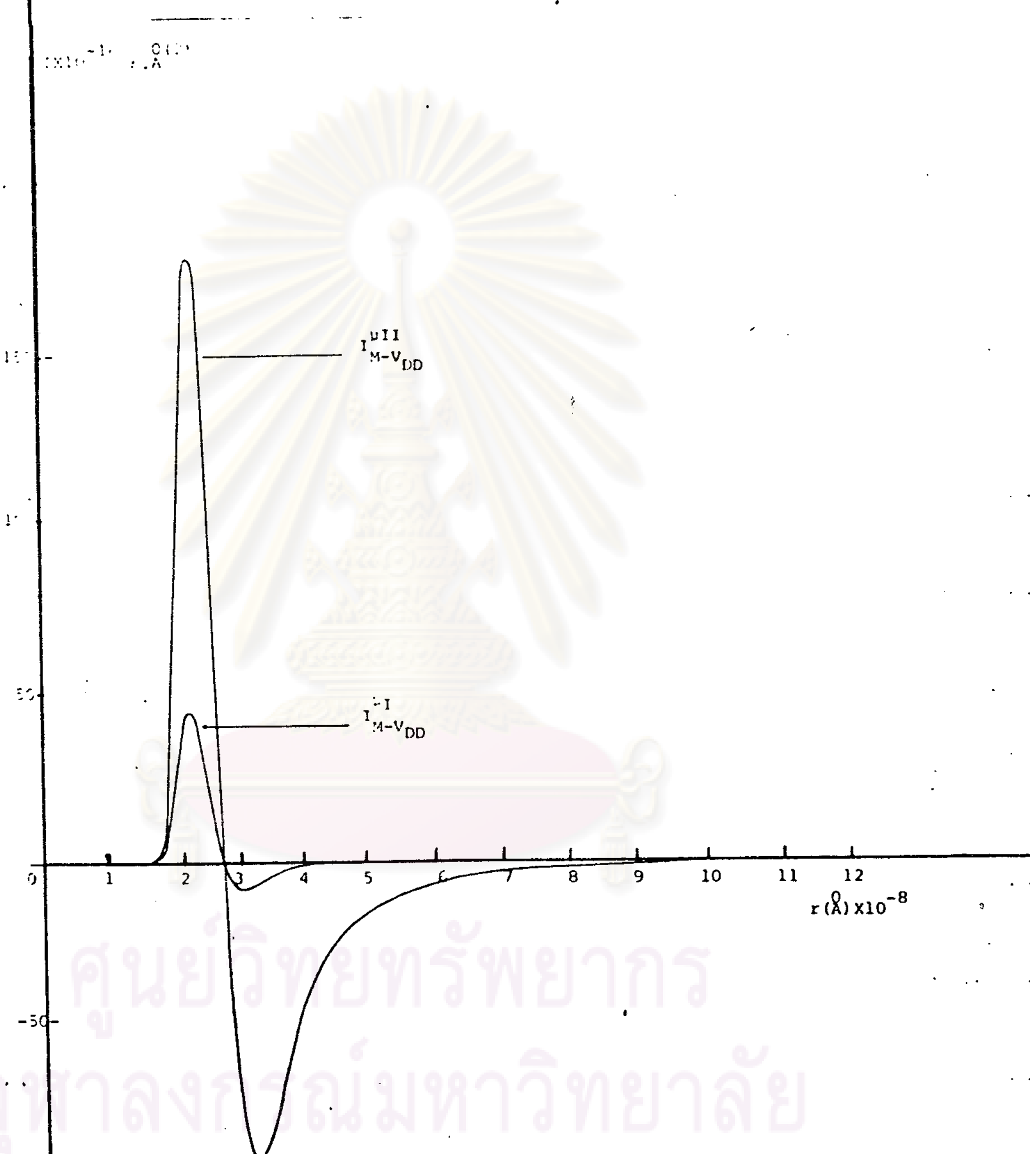

FIG 5-7 $I^{\mu I}_{M-V_{DD}}$ and $I^{\mu II}_{M-V_{DD}}$ VS r, due to the Morse-V_{DD} potential, which have been computed from McMillan's curve

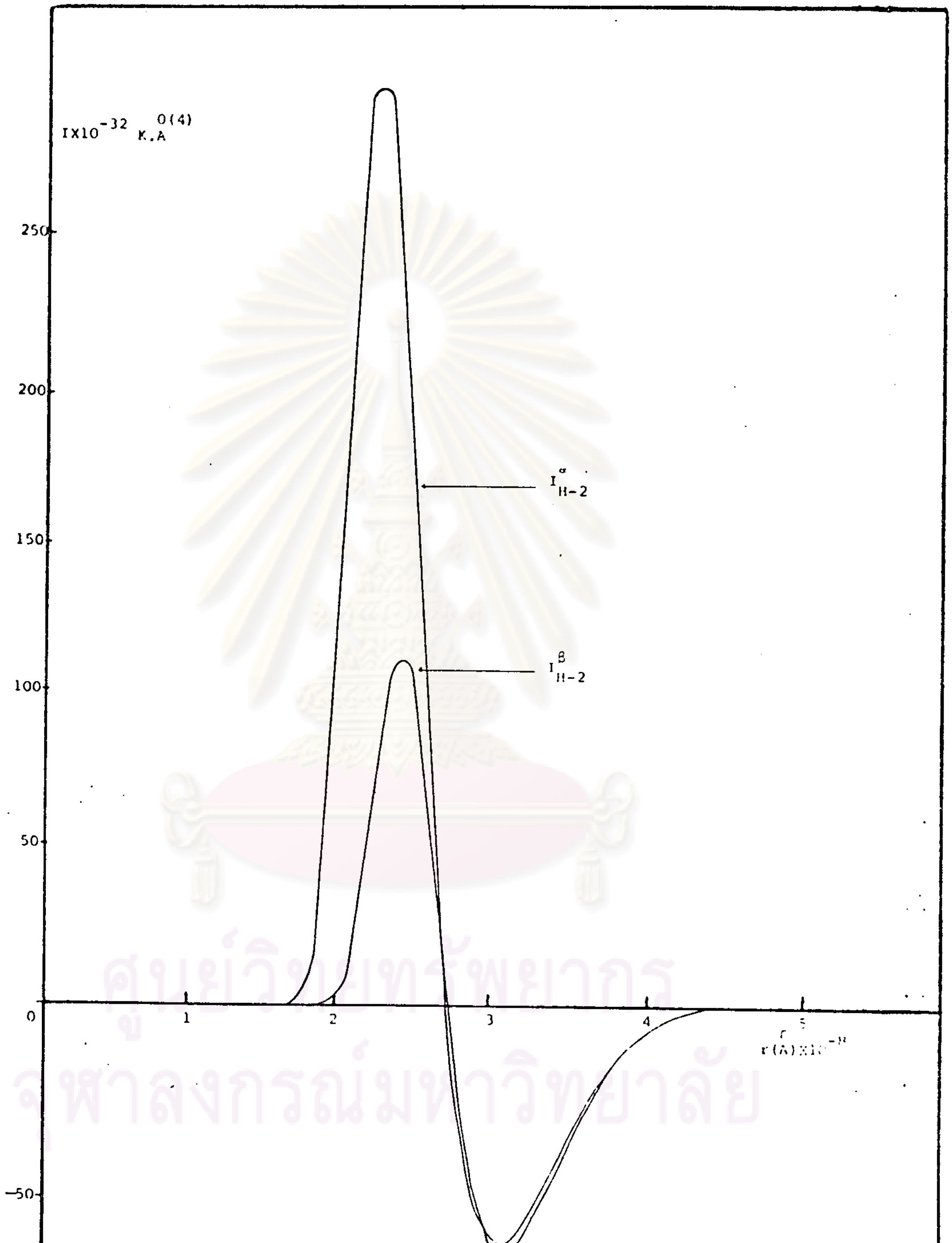

FIG. 5-8 I^{α}_{H-2} and I^{β}_{H-2} V r, due to the HFDH-2 potential, which have been computed from McMillan's curve

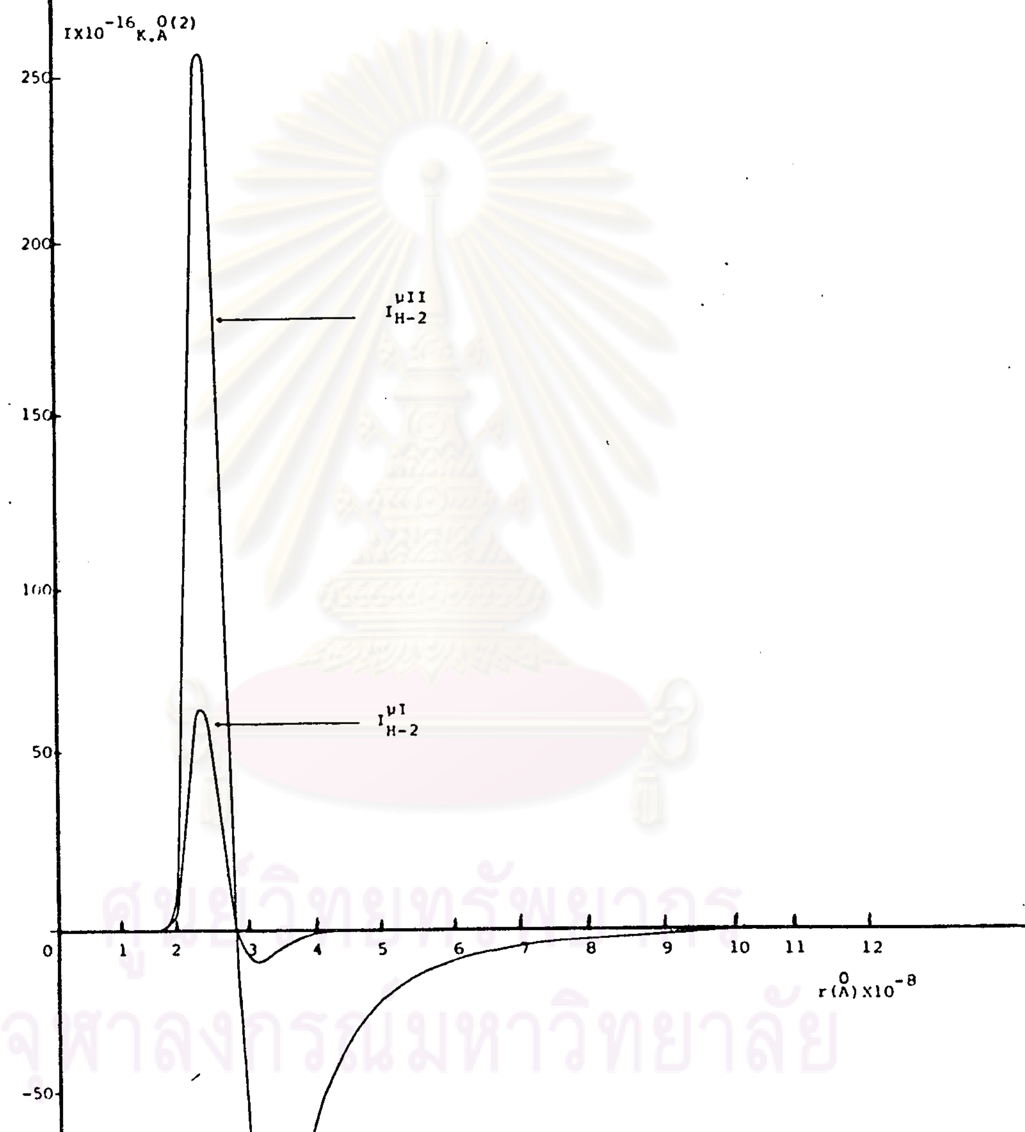

FIG 5-9 $I^{\mu I}_{H-2}$ and $I^{\mu II}_{H-2}$ VS r due to the HFDHE-2 potential, which have been computed from McMillan's curve

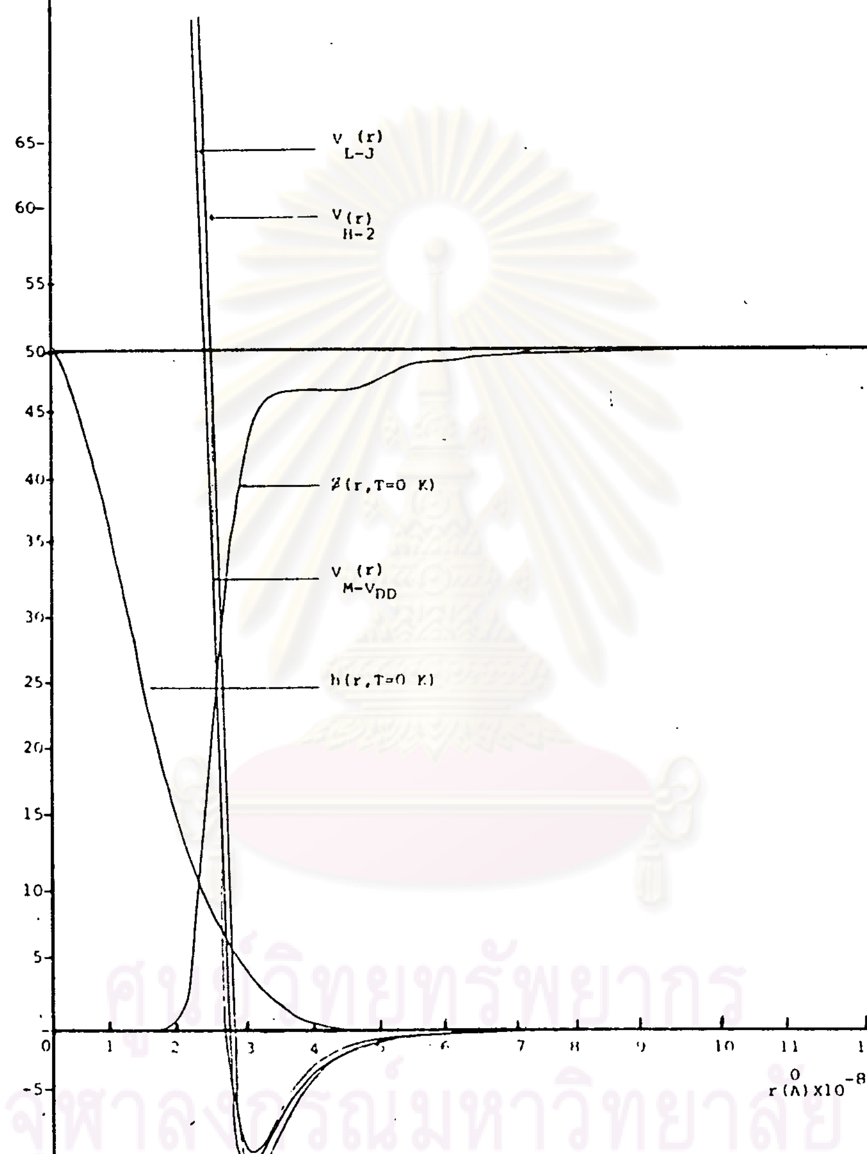

FIG 5-10 The Lennard-Jones 12-6 potential, $V_{L-J}(r)$, The Morse-V_{DD} potential, $V_{M-V_{DD}}(r)$, and The HFDHE-2 potential, $V_{H-2}(r)$, in unit of 25×10^{-2} K VS r; the screening function Ø(r,T=0 K) and the function h(r,T=0 K) VS r, computed from [illegible] scaling

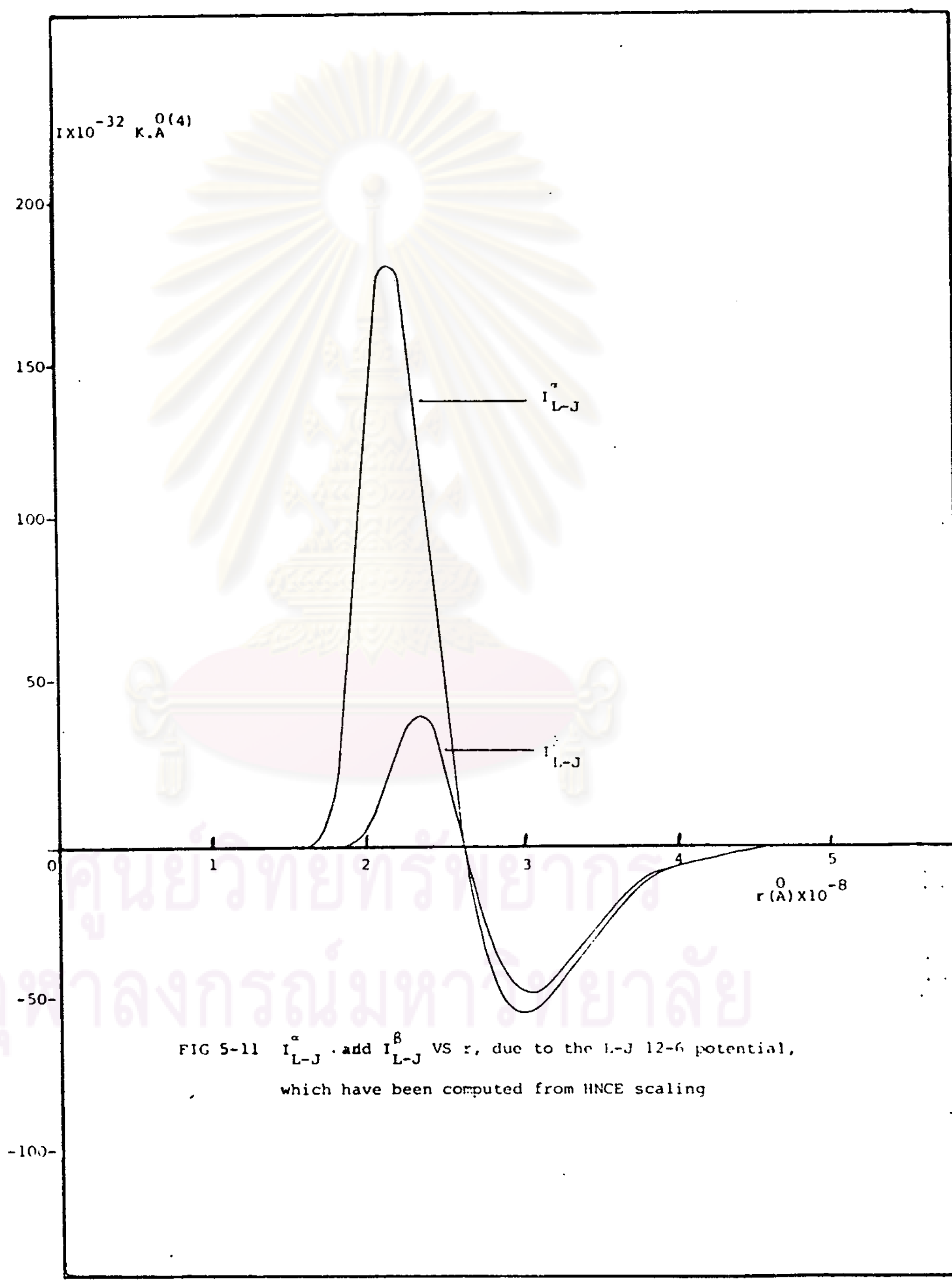

FIG 5-11 I^{α}_{L-J} and I^{β}_{L-J} VS r, due to the L-J 12-6 potential, which have been computed from HNCE scaling

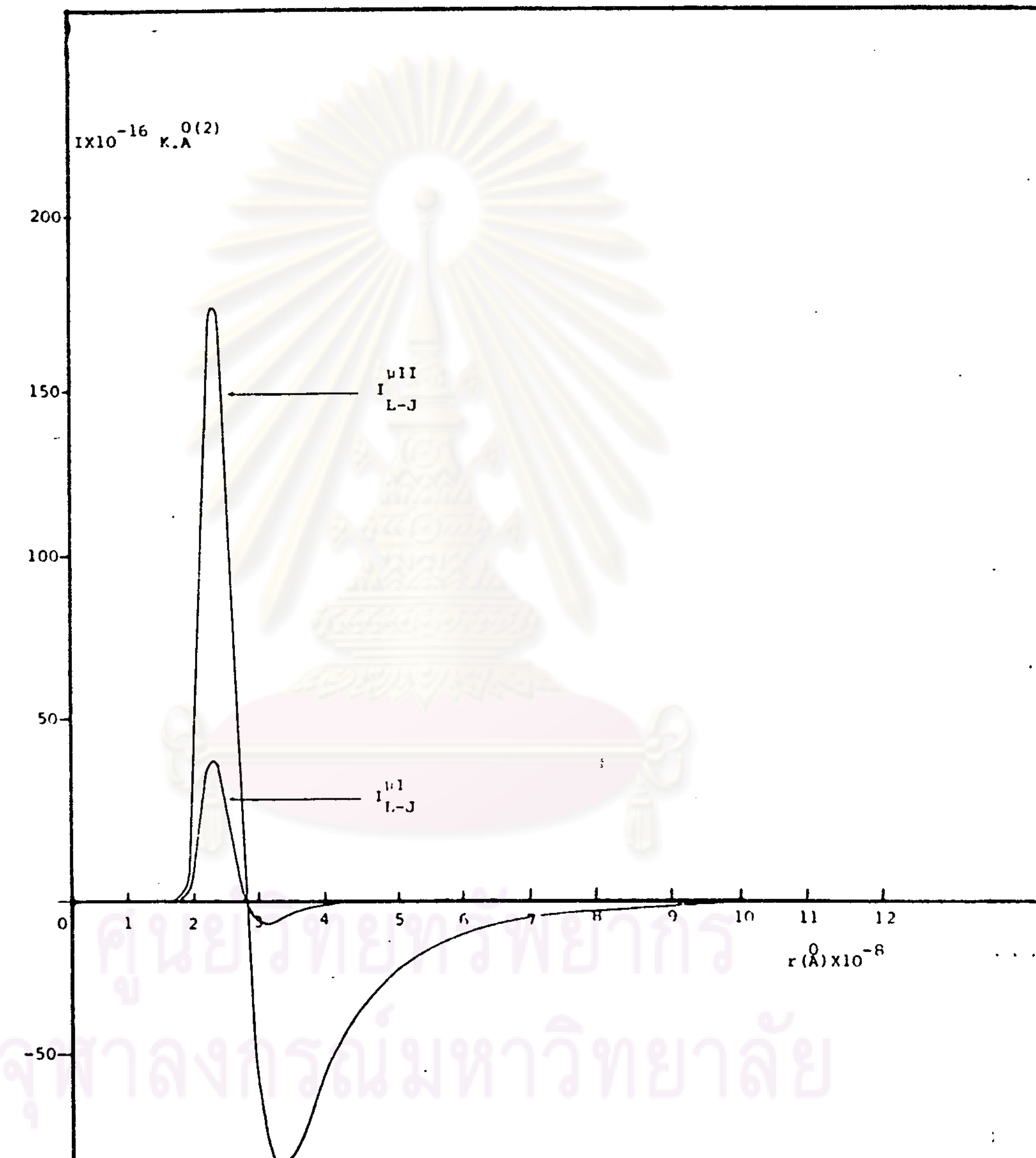

FIG 5-12 $I^{\mu I}_{L-J}$ and $I^{\mu II}_{L-J}$ VS r, due to the L-J 12-6 potential, which have been computed from HNCE scaling.

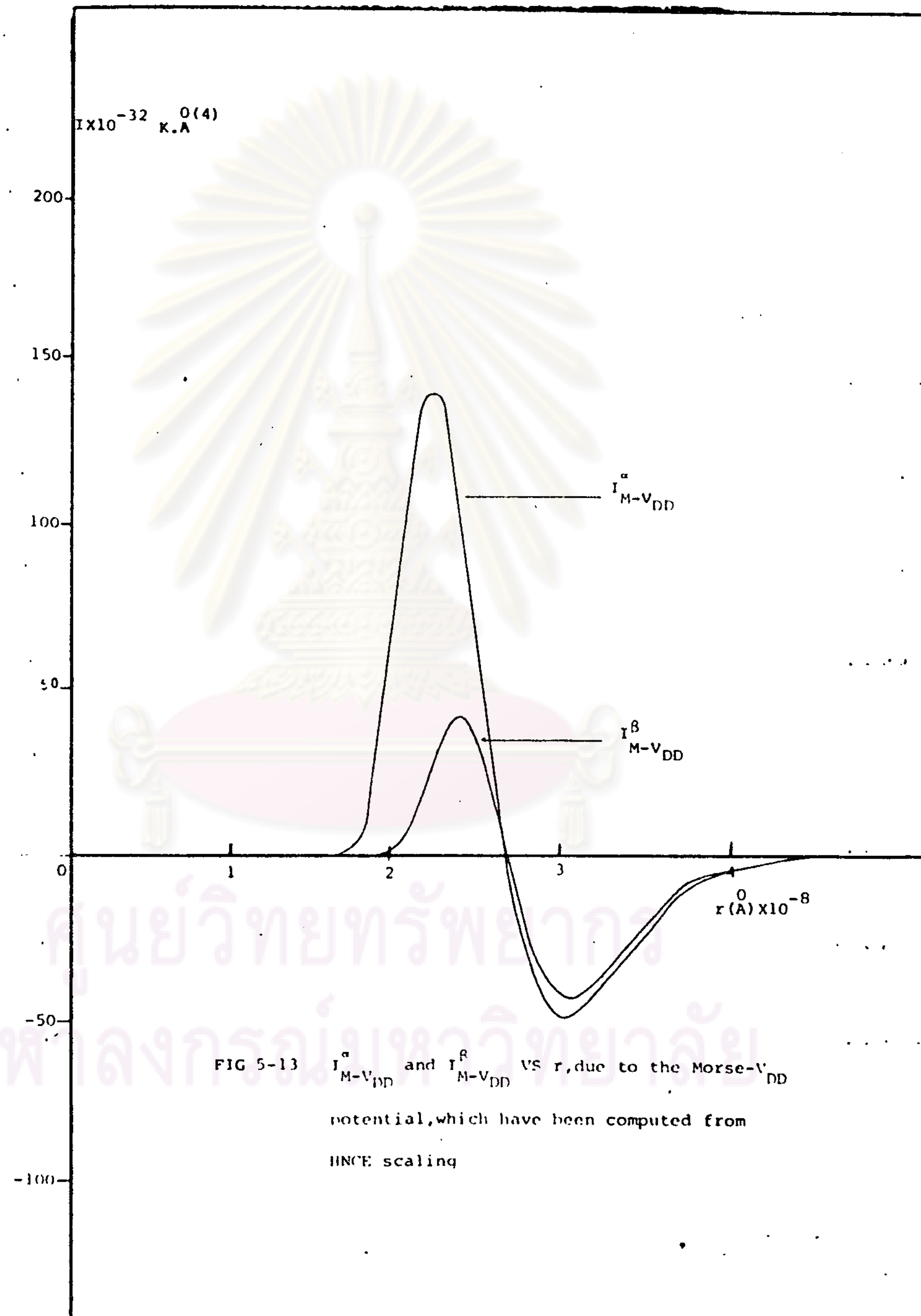

FIG 5-13 $I^{\alpha}_{M-V_{DD}}$ and $I^{\beta}_{M-V_{DD}}$ VS r, due to the Morse-V_{DD} potential, which have been computed from HNCE scaling

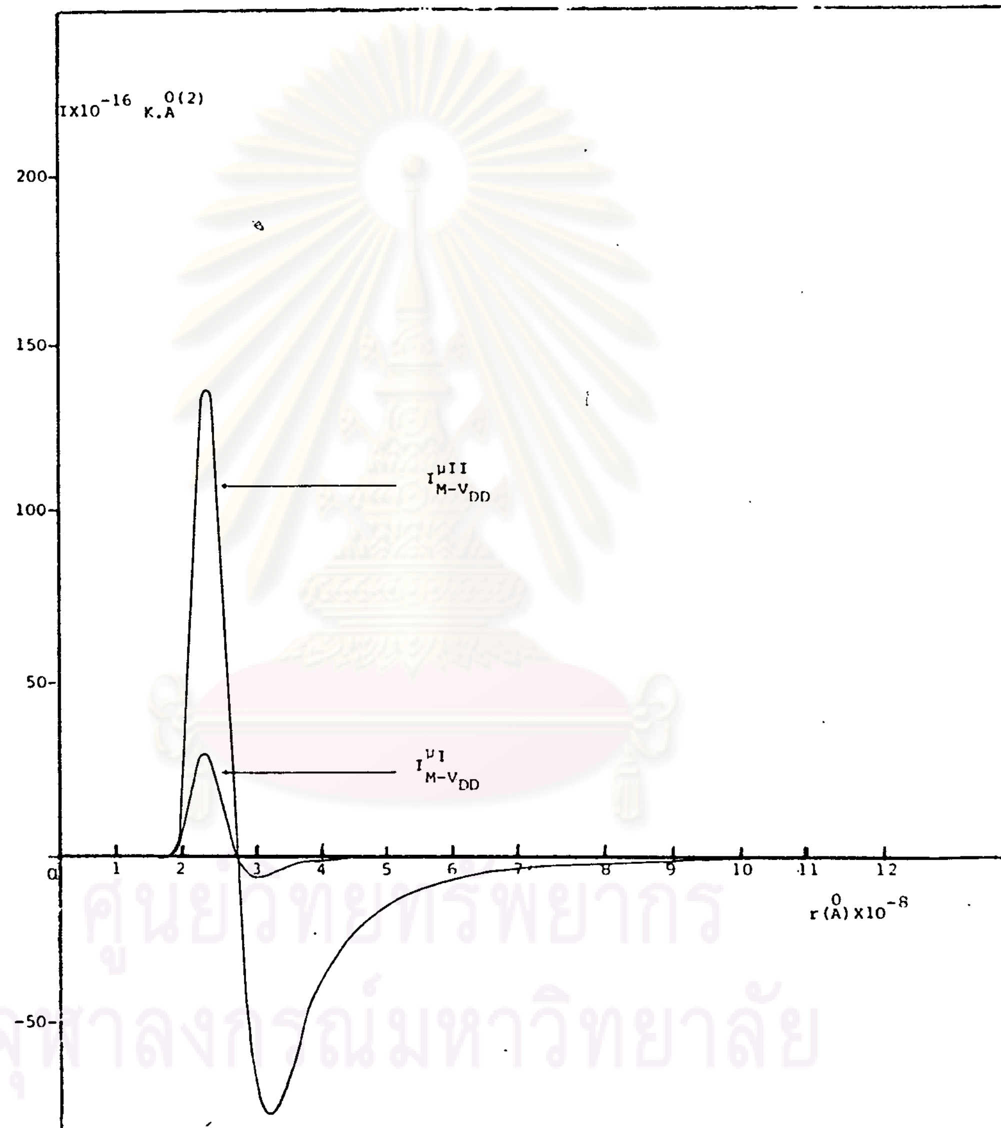

FIG 5-14 $I^{\mu I}_{M-V_{DD}}$ and $I^{\mu II}_{M-V_{DD}}$ VS r, due to the Morse-V_{DD} potential, which have been computed from HNCE scaling

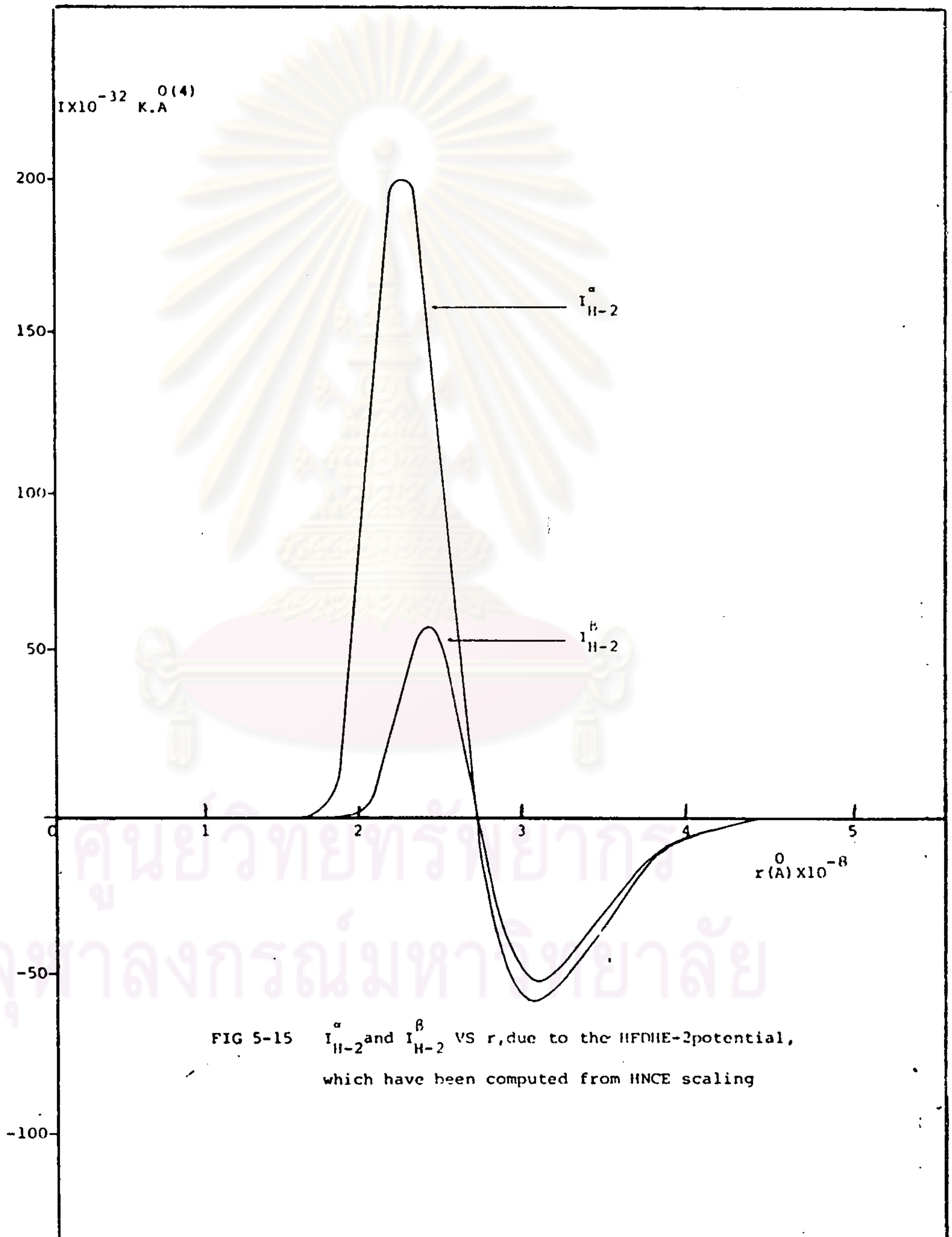

FIG 5-15 I^{α}_{H-2} and I^{β}_{H-2} VS r, due to the HFDHE-2potential, which have been computed from HNCE scaling

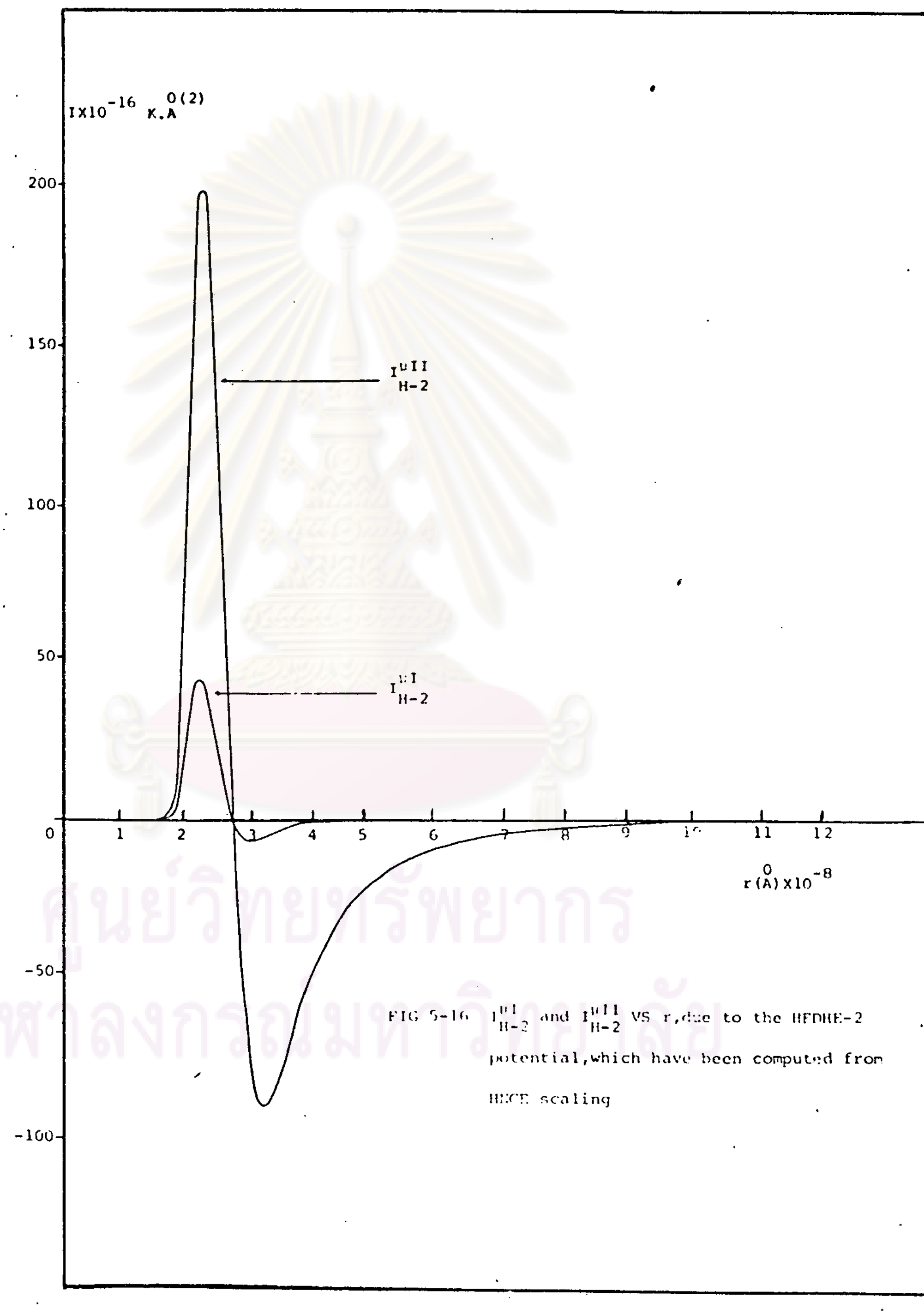

FIG 5-16 $I^{\mu I}_{H-2}$ and $I^{\mu II}_{H-2}$ VS r, due to the HFDHE-2 potential, which have been computed from HECE scaling

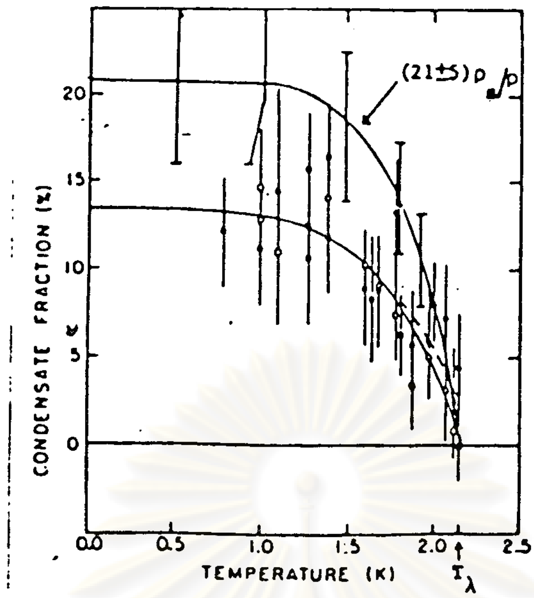

Fig.6.1 Experimental work results for the condensate fraction of superfluid ^{4}He from ref.26 (▪,•). The curve of (21±5) ρ_s/ρ comes from the theoretical calculation (29)

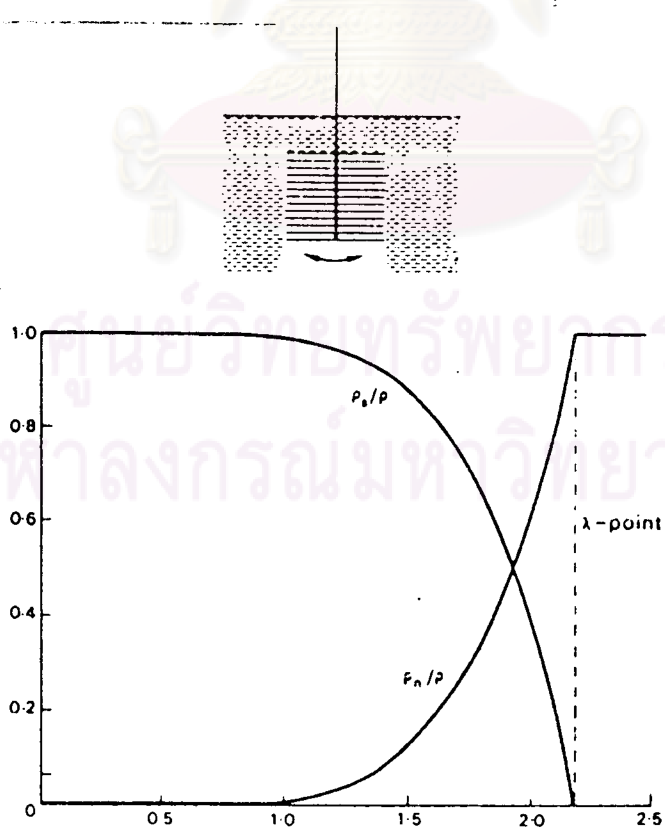

Fig.6.4 Andronikashvili's experiment

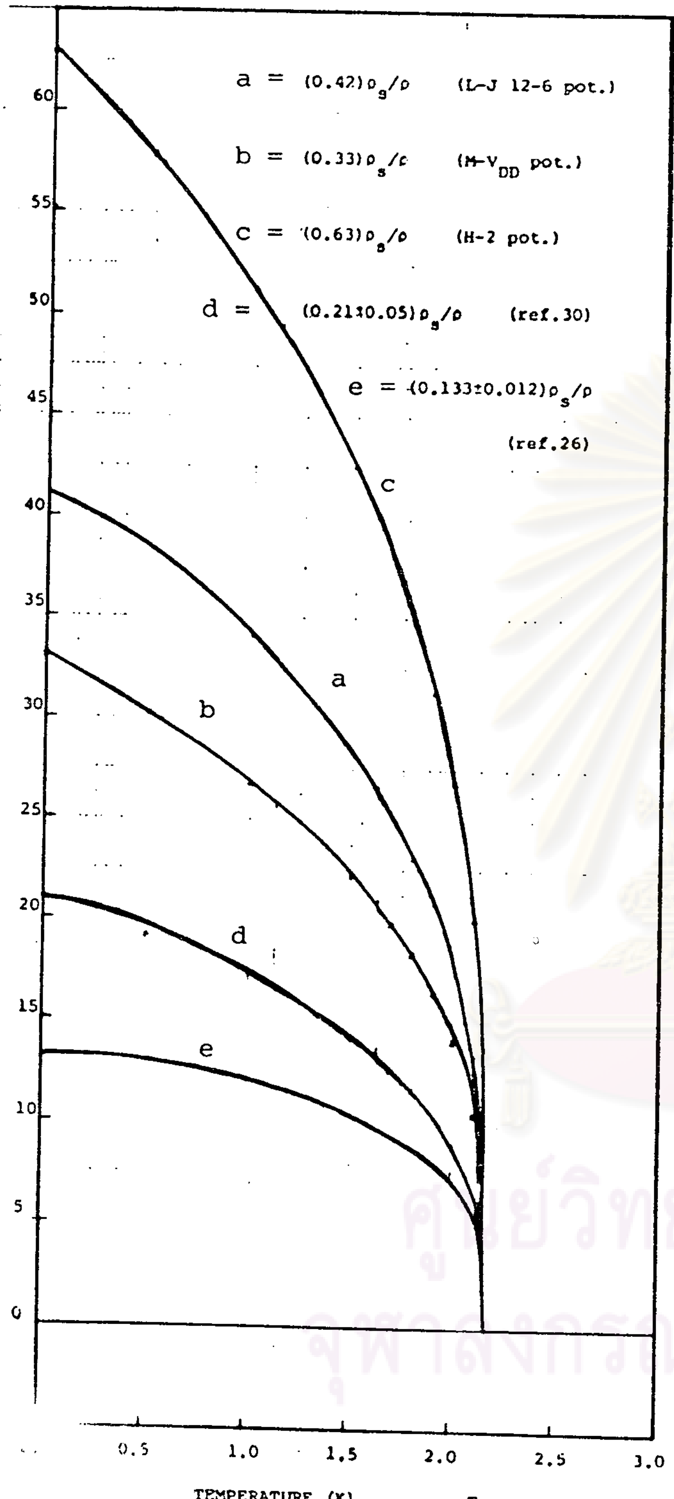

Fig 6.2 Condensate fraction of liquid ^{4}He II as a function of temperature. Smooth curve is a fit to Eq.(4-55)by using the various interatomic potential and McMillan's curve.

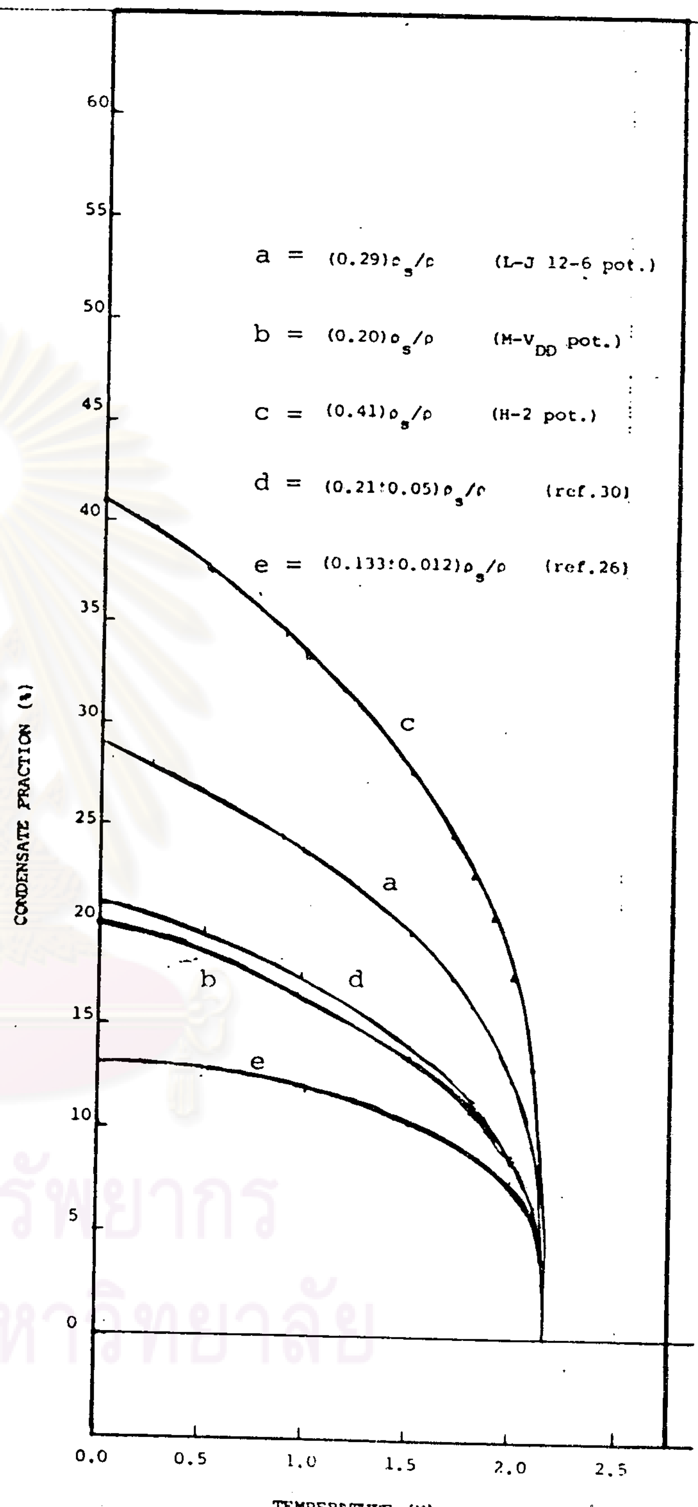

Fig 6.3 Condensate fraction of liquid ^{4}He II as a function of temperature. Smooth curve is a fit to Eq.(4-55) by using the various interatomic potential and HNCE scaling'curve.